Modulation of the spontaneous brain activity and functional connectivity in the triple resting-state networks following the visual oddball paradigm

Hasan Sbaihat[1,2,3], Ravichandran Rajkumar[1,3,4], Shukti Ramkiran[1,3,4], Abed Al-Nasser Assi[2], N. Jon Shah[1,4,5,6], Tanja Veselinović[3¶], Irene Neuner[1,3,4¶*]

[1]Institute of Neuroscience and Medicine, INM-4, Forschungszentrum Jülich GmbH, Jülich, Germanys

[2]Department of Medical Imaging, Arab-American University Palestine, AAUP, Jenin, Palestine

[3]Department of Psychiatry, Psychotherapy and Psychosomatics, RWTH Aachen University, Aachen, Germany

[4]JARA – BRAIN – Translational Medicine, Aachen, Germany

[5]Department of Neurology, RWTH Aachen University, Aachen, Germany

[6]Institute of Neuroscience and Medicine, INM-11, Forschungszentrum Jülich GmbH, Jülich, Germany

*Corresponding author

Email: i.neuner@fz-juelich.de (IN)

¶ These authors contributed equally

Abstract

The default mode network (DMN), the salience network (SN), and the central executive network (CEN) could be considered as the core resting-state brain networks (RSN) due to their involvement in a wide range of cognitive tasks. Despite the large body of knowledge relating to their regional spontaneous activity (RSA) and functional connectivity (FC) of these networks, less is known about the influence of task-associated activity on these parameters and on the interaction between these three networks. We have investigated the effects of the visual-oddball paradigm on three fMRI measures (amplitude of low-frequency fluctuations for RSA, regional homogeneity for local FC, and degree centrality for global FC) in these three core RSN networks. A rest-task-rest paradigm was used and the RSNs were identified using independent component analysis (ICA) on the resting-state data. We found that the task-related brain activity induced different patterns of significant changes within the three RS networks. Most changes were strongly associated with the task performance. Furthermore, the task-activity significantly increased the inter-network correlations between the SN and CEN as well as between the DMN and CEN, but not between the DMN and SN. A significant dynamical change in RSA, alongside local and global FC within the three core resting-state networks following a simple cognitive activity may be an expression of the distinct involvement of these networks in the performance of the task and their various outcomes.

Introduction

Examination of regional spontaneous brain activity (RSA) and functional connectivity (FC) during resting-state (RS) conditions appears to be a promising approach for understanding brain organization at the systems level [1]. Within the several stable RS networks identified up to now, three networks stand out for their importance and synchronized interplay: the default mode network (DMN), the salience network (SN), and the central executive network (CEN). These networks are often jointly referred to as the triple network model [2] and are considered to be the core neurocognitive networks due to their involvement in a wide range of cognitive tasks [1,3,4].

Specifically, the DMN is known to be a task-negative network associated with self-referential thoughts and mind-wandering [5]. It shows decreased activation during tasks in which self-referential and stimulus-independent intellectual activity is not involved [6,7]. Even more, numerous studies have demonstrated that midline DMN regions are among the most efficiently wired brain areas, serving as global hubs that bridge different functional systems across the brain [8,9]. Increased DMN connectivity with regions of other brain networks has been shown to facilitate performance during goal-directed tasks [10]. Thus, DMN is not engaged only under resting-state conditions but also under task performance and post-task processes as well [10-12].

The CEN is a task-positive network, engaged in higher-order cognitive and attention control as well as in working memory, decision making and goal-directed behavior [13-15]. Conversely, the SN is involved in detecting, filtering and integrating relevant internal (e.g., autonomic input) and external (e.g., emotional information) salient stimuli in order to guide behavior [1,16]. Furthermore, it displays a crucial role in the functional and dynamic switching between the DMN and CEN (i.e., between task-based and task-free states) [17,18].

Dynamic interactions between the three networks of the triple network model influence cognition and emotion, affecting performance and impulsivity [19-21]. Moreover, an altered interaction between these networks has been shown in patients with major depressive disorder [22], post-traumatic stress disorder [23], obsessive-compulsive disorder [24], and schizophrenia [25,26]. Altogether, an increasing body of evidence suggests that aberrant function of the triple networks underlies the psychopathology of all major psychiatric disorders [27] and disturbed functional interactions among them may be considered a potential neurophysiological biomarker for different psychopathological phenomena across several neuropsychiatric disorders [28]. It is therefore particularly important to understand the physiological fluctuations in the activity and interactions of these networks in order to be able to differentiate them from pathological conditions.

Continuous fluctuations of the main properties of the networks (as RSA and FC) have been shown during rest and during task-associated activities [29,30]. Much less is known about the extent to which these properties can be influenced by a specific task and to what extent a task-associated activity affects the interaction between the networks.

A simple method to investigate the effects of task-related activation on the RSA is the rest-task-rest paradigm (RTR) [5,31]. To date, a task-induced modulation of the RSA has been observed following cognitive tasks involving working memory, emotion, visual perception, and motor training. However, previous studies have mainly focused on whole-brain [31-35] or on specific brain structures known to be involved in the tasks [36,37]. None of the mentioned studies has specifically addressed the impact of a task on the triple network. Moreover, previous investigations have overall changes in static connectivity in different time periods (before and after the task), but changes in the relationship between the different networks (particularly in the triple network, which is the focus of this study) remain poorly understood. Thus, in this study, we have specifically examined task-induced changes in RSA and FC in the triple network of the RS (DMN, SN and CEN) and the task-induced effects on the interactions between them.

Concretely, this study aims to assess the extent of the influence exerted by a well-established task - the visual oddball paradigm [38] on the post-task RS in the regions of the triple network using the RTR design. The visual oddball paradigm task was chosen as it elicits the blood oxygen level dependent (BOLD) response in a large set of distributed networks [39-43]. In particular, the task performance is associated with activation in brain regions linked to the three networks (the SN [44], the dorsolateral prefrontal cortex (CEN) [45,46], and the cingulate and prefrontal cortex (DMN) [47].

For the identification of the triple network regions we applied a group independent component analysis (ICA) to the RS data. Several different measures of FC can be calculated from fMRI, each reflecting a different property of the brain networks. For this approach, we chose two such measures, the regional homogeneity (ReHo) [48] the degree centrality (DC) [49], as these are suitable for investigating the voxel level local and global FC, respectively. Furthermore, the amplitude of low-frequency fluctuations (ALFF) [50], is suitable for depicting the RSA. Combining these measures enables the complementary characterization of changes in activation and communication of specific networks or regions.

We hypothesised that the task-based activity would distinctly affect the RS RSA as well as the local and the global connectivity in the triple network. Due to the central role of the SN during the occurrence of salient stimuli or during the performance of a cognitive task, we also expected internetwork functional connectivity to increase between the SN and the other two networks of the triple network model (DMN, CEN).

Materials and Methods

Subjects

21 right-handed healthy subjects (17 males and four females) were included in this study (age range between 19 to 40 years; mean: 29 ± 5.6 years). All subjects were healthy and without a history of neurological or psychiatric disorders. The study was approved by the Ethics Committee of the Medical Faculty of the RWTH Aachen University, Germany. Written informed consent was obtained from all subjects following the recommendations of the Declaration of Helsinki.

Experimental design

To investigate the effects of task-induced brain activity on the post-task resting-state, the experiment followed a rest-task-rest (RTR) design consisting of three parts – each part representing a different brain state: first RS (R1), active state (during the performance of the visual oddball paradigm) and the second, post-task RS (R2) (Fig 1).

Fig 1. Experimental design of the rest-task-rest paradigm (RTR) which includes two resting-state conditions (pre- and post-task resting-state, R1 and R2) and the task condition composed of three subtasks of the visual oddball paradigm (VOP).

During RS conditions, the subjects were instructed to close their eyes and not focus on any specific thoughts. All the fMRI data were acquired in a single scanning session and instructions were given to the subjects in-between each condition via a microphone.

The visual oddball paradigm comprises of three subtasks: passive (T1), count (T2), and respond (T3). Two different colored circles were established as frequent (yellow circles) and target (blue circles) stimuli. During the passive condition, the subjects were asked to simply keep the stimuli under observation. During the count condition, the subjects were asked to count the target stimuli (blue circles), and during the respond condition, the subjects were instructed to press a button with their right index finger as soon as they recognised the target stimuli.

Each visual oddball paradigm condition included 200 trials (160 frequent and 40 target stimuli). The single stimulus was 30 cm in diameter shown on a black background for 500 milliseconds with a variable interstimulus interval (ISI) of 500–10,000 milliseconds. The stimulus generator board (ViSaGe MKII, Cambridge Research System Ltd.) was used to generate the stimuli and a thin-film transistor display was used to view the stimuli. The thin-film transistor display was installed behind the scanner and was viewed using a mirror placed on the head coil of the magnetic resonance (MR) scanner.

A part of this data set (N = 16), which mainly focused on the analysis of the effects of different response modalities on the fMRI BOLD activation during the visual oddball paradigm, has been published previously [51].

MR Data Acquisition

MR data were acquired using a 3T scanner (TIM-Trio, Siemens Healthineers, Erlangen, Germany). Sponge pads were used to reduce motion artefacts by limiting the subject's head movement. The fMRI data were acquired using an echo planner imaging (EPI) sequence. The number of volumes were 304 for each task and 180 for each RS condition (repetition time (TR) = 2000 ms, echo time (TE) = 30 ms, flip angle (FA) = 79°, field of view (FOV) = 200 × 200 mm, 64 × 64 matrix, slice thickness = 3 mm, number of slices = 33).

Structural images were acquired using a magnetization prepared rapid gradient echo (MP-RAGE) sequence (TR = 2250 ms, TE = 3.03 ms, FA = 9°, FOV = 256 × 265 mm, 64 × 64 matrix, 176 slices, voxel size 1 × 1 × 1 mm^3).

fMRI Data Analysis

Task Data

The analysis of the task-related brain activation was performed using FSL software package (FMRIB's Software Library, www.fmrib.ox.ac.uk/fsl). The pre-processing included slice timing correction, brain extraction (using BET) [52], motion correction (MCFLIRT) [53], spatial smoothing using a Gaussian kernel of full width at half maximum (FWHM) of 5 mm, and high pass temporal filtering (100s). A time-series of BOLD signal based on the general linear modal for each individual data set was performed using FILM with local autocorrelation correction [54]. The functional images were registered to the high-resolution structural images and subsequently to the Montreal Neurological Institute (MNI) standard space using the FLIRT tool [55]. The first-level analysis was performed with two explanatory variables (EV). The EVs were convolved with a double-gamma hemodynamic response function (HRF). Four contrasts were then created: target stimuli, frequent stimuli, target > frequent, frequent > target.

Group-level mixed-effects analysis was performed for the passive, count and respond sub-tasks to create a mean for each first level contrast using FLAME with spatial normalization to MNI space and using a cluster with a significance threshold of $Z > 2.3$, $p = 0.05$ [56]. A tripled two-group difference ("tripled t-test") Was performed to evaluate the additional activation added to the passive condition by the count and respond conditions. The activation pattern regions were defined using Harvard-Oxford Cortical Structural Atlas in FSL software (FMRIB, Oxford, UK).

Triple network identification

The multivariate exploratory linear decomposition into independent components (MELODIC) tool from the FSL software package was used to identify the triple networks (DMN, CEN, and SN) using pre-task RS fMRI data. Subject level RS-fMRI data were pre-processed as follows: the first eight fMRI volume images were removed, followed by slice timing correction, brain extraction (BET) [52], motion correction (MCFLIRT) [53], spatial smoothing FWHM = 5 mm, and high-pass temporal filtering 125s. The functional MRI images were co-registered linearly to high-resolution structural images and nonlinearly to MNI standard space using FLIRT [55]. Group ICA analysis was used to decompose the pre-task RS data into 20 components.

To identify the triple networks, a cross-correlation was performed between the functional brain networks atlas [57] and each of the ICA components. The cross-correlation was performed using the FSLUTILS (https://fsl.fmrib.ox.ac.uk/fsl/fslwiki/Fslutils) tool implemented in the FSL software package. ICA components that showed maximum correlation with each of the three networks in the functional brain networks atlas were chosen. The identified brain networks were binarized and used in the subsequent analysis as masks. The binarized masks were corrected for grey matter (GM) by including the voxels which showed more than 50% probability of being

GM. The GM correction was performed using a tissue segmented MNI152 (2 × 2 × 2 mm^3) template.

fMRI measures calculation

The fMRI measures were computed for both the tasks and RS-fMRI using data processing and analysis for brain imaging (DPABI) [58], and SPM12 (http://www.fil.ion.ucl.ac.uk/spm/) toolboxes built on MATLAB software package version 2017b (The Math Works, Inc., Natick, MA, USA). Pre-processing was performed using the data processing assistant for the RS-fMRI (DPARSF) [59] advanced edition as follows: first eight fMRI volume images of each condition in each subject's dataset were removed, followed by slice timing correction, realignment, nuisance covariates regression (NCR) and temporal filtering between 0.01 and 0.08 Hz. To get rid of the nuisance signals, the Friston 24-parameter model was used for covariate regression. The fMRI measures were calculated for each subject separately in individual brain imaging space. The DC was computed by applying a Pearson correlation coefficient between the time series of a given voxel and all other voxels in the whole brain by thresholding each correlation at ($r > 0.25$, $p \leq 0.001$) [60]. ReHo was calculated by estimating the synchronization or similarity between the time series of a given voxel and 26 nearby neighbor voxels [48] using Kendall's coefficient of concordance (KCC) [61]. The ALFF was calculated within the low-frequency range (0.01 – 0.1 Hz) [62]. The fMRI measures were normalised using a Z-value standardization procedure by subtracting the mean from each voxel and then dividing the value by the standard deviation of the whole brain. The Z-value standardised measures were co-registered to the MNI standard space (2 × 2× 2mm^3), and, finally, spatial smoothing with FWHM at 4mm^3 was performed.

Further calculated values

The fMRI measures ALFF, ReHo, and DC were extracted from all voxels of the triple network for each condition in all subjects using the binarized triple network masks. The extracted voxel-level values were used to calculate several parameters of interest, relevant for the examination of the task effect on the post task resting-state. These parameters and the exact description of how they were calculated are shown in Table 1.

Table 1: Description of parameters used to examine the effect of the task on the fMRI measures in the post-task RS

Parameter	**Calculation procedure/ meaning**
R1	Voxel-level fMRI measures during the first (pre-task) resting-state (RS) (baseline)
R2	Voxel-level fMRI measures during the second (post-task) RS.
T1, T2, T3	Voxel-level fMRI measures during the three subtasks of the visual oddball paradigm.
RS difference (RSD)	Difference between post- and pre-task RS (R2 - R1) in the voxel-level fMRI measures for each subject.
Task $_{(whole)}$	Task $_{(whole)}$ = (T1 + T2 +T3) / 3 (mean values of the fMRI measures during the three subtasks)
Main task $_{(whole)}$	Task $_{(whole)}$ - R1
RS similarity (RSS)	Correlation coefficient between R1 and R2 for each subject.
Task effect at the group level	Correlation coefficients between the differences (Task (whole) – R1) and (R2 - R1). All correlation coefficients were computed using Pearson's correlation coefficients at a significance level of $p < 0.05$.

The inter-network FC of the three networks were calculated by first extracting the mean of the BOLD signal time series from the binarized mask of each network, followed by the computation of the Pearson's correlation coefficient between each pair of networks. Fisher r to z transformation was performed to improve the normal distribution. A paired t-test was used to examine the difference of FC between the pre- and the post-task RS.

To investigate the relationship between the behavioral data (e.g. reaction time) and the fMRI measures, the correlation coefficients between the RSD and subject's reaction time in the response condition was performed. Having checked the normality of the data using the Kolmogorov-Smirnov test, a paired-sample t-test was used in order to find the differences between the pre- and post-task RS in each fMRI measure.

Results

Behavioural data

The mean reaction time of the respond condition was 477ms (SD = 13).

Imaging data - task data

The task data were initially analysed and reported following the examination of the first 16 participants [51]. The current analysis includes an enlarged collective of test subjects (N = 21) and confirms previously reported findings. In summary, activation in regions associated with a response to visual stimulation (occipital cortex) for both the target and the frequent stimuli was observed during all three subtasks of the visual oddball paradigm. Both, the count and respond conditions differed significantly from the passive condition in a number of brain regions including the pre- and post-central gyri, regions of the parietal cortex and the middle and inferior frontal gyri. Compared to the count condition, the response contrast yielded significant differences in the parietal operculum, inferior parietal lobule, insula, anterior cingulate cortex, and the posterior cingulate cortex (PCC).

Imaging data -Triple network resting-state data

The triple network was identified using group independent component analysis (Fig 2). Specifically, the DMN included the posterior cingulate cortex (PCC), precuneus, angular gyrus, and medial prefrontal cortex (mPFC); the CEN included the lateral posterior parietal cortex (LPPC) and dorsolateral prefrontal cortex (DLPFC); the SN included the frontal insular cortex (FIC), and anterior cingulate cortex (ACC).

Fig 2. Depiction of the triple networks referred to as the triple network: default mode network (DMN, blue colour), central executive network (CEN, red colour), and salience network (SN, green colour). The networks were identified by decomposing the pre-task resting-state condition into 20 components from 21 subjects.

RSA and FC across different brain-states

The fMRI measures showed different values in the RSA and the local and global FC during the different brain-states (rest-task-rest) (Fig 3). These values differed significantly at the group level. A pairwise comparison between the pre- and post-task RS (R1 and R2) revealed significant differences in each network and for each fMRI measure at a significance level of $p < 0.05$, with exception of the ReHo measure in the SN (Table 2).

Fig 3. fMRI measures (ALFF, ReHo, and DC) from 21 subjects. Visual inspection shows a change in each of the three fMRI measures in the post-task resting-state (R2) when compared to pre-task resting-state networks (R1). The differences between R1 and R2 were

significant in each network and in each fMRI measure at significance level $p < 0.05$, with exception of the ReHo measure in the salience network (SN).

Table 2. A paired-samples t-test was performed to compare the pre-task resting-state (R1) and post-task resting-state (R2) conditions in the triple network (default mode network (DMN), salience network (SN), and central executive network (CEN)), in each fMRI measurement (21 Subjects). There was a significant difference of $p < 0.05$ between R1 and R2 in each network and in each fMRI measurement, with the exception of the SN from the ReHo measurement.

Brain network	**Mean values in R1**	**Standard deviation of values in R1**	**Mean values in R2**	**Standard deviation of values in R2**	**P-Value**	**T-Value**
Amplitude of low frequency fluctuations (ALFF)						
DMN	0.1935	0.3429	0.1120	0.3344	0.0000	22.33
CEN	0.1592	0.3690	0.0420	0.3569	0.0000	20.92
SN	-0.0475	0.3207	-0.0787	0.3151	0.0000	10.17
Regional homogeneity (ReHo)						
DMN	0.8096	0.6722	0.8333	0.6511	0.0161	2.40
CEN	0.7172	0.5942	0.5955	0.6045	0.0000	9.01
SN	0.0936	0.4972	0.0809	0.4908	0.1431	1.46
Degree centrality (DC)						
DMN	0.1278	0.3705	0.1154	0.3628	0.0280	2.19
CEN	0.2673	0.3669	0.2231	0.3295	0.0000	5.69

SN	0.0276	0.3269	0.0726	0.3250	0.0000	9.71

Concretely, the ALFF values decreased significantly in all three observed networks ($p < 0.001$ in all three networks). For the local connectivity parameter (ReHo), a significant increase in the DMN ($p = 0.016$) was observed, while the ReHo value decreased in the CEN ($p < 0.001$) and remained without statistically significant alteration in the SN. The long-range connectivity (DC) decreased significantly in the DMN and CEN ($p = 0.028$; $p < 0.001$), while increasing in the SN ($p < 0.001$).

Associations between the pre- and post-task resting-state differences and the task

The RSS values were calculated separately for the triple networks (DMN, CEN and SN) for each of the fMRI measures (ALFF; ReHo and DC) are shown in Table 3. The RSS values were comparable for all three parameters across all three networks.

Table 3. Mean values, standard deviation, and the range of the resting-state similarity (RSS) calculated separately for each resting-state fMRI parameter (ALFF, ReHo, and DC) and for each of the triple networks (default mode network (DMN), salience network (SN), and central executive network (CEN).

	RSS (Mean)	RSS (SD)	RSS (Range)
DMN			
ALFF	0.8818	0.029	0.824 – 0.925
ReHo	0.8118	0.039	0.698 - 0.876

DC	0.7563	0.0657	0.575 - 0.884
CEN			
ALFF	0.8736	0.044	0.763 - 0.946
ReHo	0.7788	0.051	0.655 - 0.867
DC	0.7574	0.097	0.425 - 0.864
SN			
ALFF	0.8855	0.048	0.721 - 0.934
ReHo	0.7583	0.045	0.664 - 0.851
DC	0.7561	0.083	0.498 - 0.880

The correlation between the differences between post-task and pre-task RS parameters (RSD = R2 - R1) and the fMRI measures resulting from the pure task effects (task $_{(Whole)}$ - R1) are depicted in (Fig 4). Significant positive correlations were found in DMN for ALFF (r = 0.48, p = 0.02) and DC (r = 0.58, p = 0.005); in CEN for ALFF (r = 0.44, p = 0.04), ReHo (r = 0.69, p = 0.004) and DC (r = 0.67, p = 0.008); and in SN for ALFF (r = 0.69, p = 0.004), ReHo (r = 0.58, p = 0.004), and DC (r = 0.49, p = 0.02).

Fig 4. Correlations between the fMRI measures resulting from the pure task$_{(whole)}$ effects and the RSD in the triple network, including the DMN, CEN, and SN of the fMRI measures.

Further, a significant negative correlation was observed between the RS differences (RSD) in DC and the subject's reaction time in the respond condition in the SN (r = -0.46, p =

0.04), but not in ReHo or ALFF measurements. No significant correlations between the fMRI measurements and the reaction time could be observed in DMN and CEN (Fig 5).

Fig 5. Correlation between the resting-state differences (RSD) and the subject's reaction time to the respond condition of the VOP, depicted in the triple networks and each fMRI measurement. Only the SN shows a significant negative correlation in the DC measurement.

Inter-network interaction

The functional connectivity between the DMN and CEN increased significantly following the performance of the task ($p = 0.015$). The connectivity strength between the DMN and the SN remained stable ($p = 0.25$), whereas it increased significantly between the SN and CEN ($p = 0.0004$) (Fig 6).

Fig 6. Strength of the FC between each pair of networks in the triple network in the pre- and post-task resting-state. There is a significant increase in FC between the DMN and CEN, and between the CEN and the SN in the post-task resting-state ($p < 0.05$). The bars represent the standard error.

Discussion

In this study, we investigated the effects of a simple visual-oddball paradigm on three basic fMRI measurements of the RS – ALFF (RSA), ReHo, and DC (the local and the global functional connectivity, respectively) - in the three networks - DMN, CEN, and SN. Our analysis revealed that the brain activity following completion of the task had a significant effect on all examined parameters in all networks, except for the measure of local connectivity (ReHo) in the SN. Furthermore, the task performance induced a significant increase in the inter-network correlations between the SN and CEN, as well as between the DMN and CEN, but not between the DMN and SN. Also, the differences between the pre- and the post-task RS (R2 - R1) were strongly associated with the main task influence ($task_{(Whole)}$ - R1) in all three networks (ALFF and DC in the three networks, ReHo in the CEN and SN). Finally, at a behavioral level, the task performance (subject's reaction time in the respond condition) correlated solely with the RS difference in DC for the SN.

Our findings indicate dynamic, disparate alterations in the post-task resting-state brain networks as a function of immediately preceding cognitive experiences. Thereby, the extent of the changes in the RS networks can be said to be closely associated with the magnitude of the direct task-effects measurable during the task performance.

Within the DMN, the ALFF values decreased significantly, indicating a reduction of the DMN RSA following task performance. This effect has been reported previously [63-65]. As the DMN is regularly deactivated during the task performance [66,67], the continued reduction of the RSA observed after the task could be an expression of a redistribution of cognitive resources in the subsequent rest phase but could also indicate a neuronal correlate of task-induced temporal fatigue after a cognitive engagement [64]. In our study, the ALFF decrease in the DMN was accompanied by a decrease in DC. Similar findings have been previously reported after subjects performed a sustained auditory working memory task [65]. Interestingly, the local FC (ReHo) increased significantly in the DMN. Local FC is defined by the temporal coherence or synchronization of the BOLD time series within a set of a given voxel's nearest neighbors [26]. ReHo represents the most efficient, reliable, and widely used index of local FC [68,69]. An increase in ReHo indicates an increased local synchronization of spontaneous neural activity [65]. Moreover, it was previously postulated that ReHo correlates with measures of functional segregation such as local efficiency and clustering coefficients [70]. Thus, increased ReHo in the DMN following task completion may reflect a restriction of information transfer to spatially close areas, as well as functional segregation from distant hubs and decreased communication with remote brain regions [71]. This result complements the observation of the decreased DC values in the post-task RS in DMN.

A significant increase in global brain connectivity (DC) was found in the SN in the post-task RS. This finding is in concordance with the established role of the SN as a network known to demonstrate competitive interactions during cognitive information processing [6,19] and, thus, having a critical role in switching between two other major RS networks (the DMN and the CEN [1]. In particular, the main hubs of the SN, the frontal inferior insula and ACC, are known to share significant topographic reciprocal connectivity and form a tightly coupled network, ideally placed to integrate information from several brain regions [72,73]. Thus, they seem to moderate arousal during cognitively demanding tasks and play a unique function in initiating control signals that activate the CEN and deactivate the DMN [74].

The finding of a significant decrease of the RSA (ALFF) in the post-task RS in SN is slightly more complex to explain. Previous investigations have linked increased ALFF values in some parts of the SN to a hyperarousal state in patients with MDD [75]. The reduction of the RSA in the post-task RS in our study may be an expression of a decreased arousal and decreased stimulus monitoring immediately after a completion of a task.

The connectivity analysis between the three networks revealed an increased synchronization (in terms of a significantly increased connectivity strength) for the SN with the CEN but not with the DMN in the post-task RS compared to the pre-task RS. This may be an after-task of the inter-network interactions during the paradigm performance. Indeed, Sridharan and colleagues have shown that the connectivity strength during the visual oddball paradigm particularly increased between the main nodes of the SN (frontal anterior insula and ACC) and all main nodes of the CEN, while the interactions between the SN and DMN were less pronounced [74].

In the CEN, the spontaneous brain activity (ALFF) decreased alongside the measures of the local and global connectivity. At a broad level, the CEN is included in higher order executive functioning, including the cognitive control of thought, emotion regulation, and working memory [16,76,77] and is thus activated during efforts to exert self-control, reappraise threatening stimuli, and to suppress intrusive, unpleasant thoughts [78-80]. CEN activity has been shown to be anti-correlated with activity in the DMN in healthy adults [1,19,74], while some investigations indicate that the CEN also exhibits an inhibitory control on the DMN [81]. Thus, the decrease in RSA in the CEN following completion of a cognitive paradigm may be the basis for the restoration of the regular activity of the DMN within the scope of a decline in DMN inhibition which occurred as a result of increased CEN activity during the task performance.

Interestingly, the connectivity between the CEN and DMN also increased in the post-task resting-state. This finding is consistent with the literature on the cooperative activity of the DMN and the CEN during different mental operations [82]. An increased coupling between some parts of these two networks has been shown in problem-solving tasks [83], social working memory [84], and during creative idea production [85]. Furthermore, a significant interaction between the DMN and the CEN has also been shown during the RS condition [86]. Thereby, this interaction seems to fluctuate dynamically across short time scales [87], indicating that the temporal relationships between the DMN and CEN shifts depending on the change in the attention focus and the immediately preceding activity. Thus, the increased connectivity between the DMN and the CEN in the post-task RS observed in our study may be an expression of the shifting of attention after task completion.

Several subregions of the triple networks are known to be activated during the performance of cognitively demanding tasks [88]. In the case of the visual oddball paradigm performed in our study, the main task specific activation has been reported previously by Warbrick and colleagues [51]. The target detection specifically involved parts of the DMN (PCC) and the SN (Insula, ACC). The insula activation was common to the count and respond conditions. The intensive involvement of different subregions of the triple networks in the performance of the task may have contributed to the significant changes in the triple network model networks in the post-task RS compared to the pre-task RS. Indeed, we have found positive correlations between the extent of the differences between R1 and R2 regarding specific parameters and the actual task effect on the same parameters in the triple networks. These correlations were significant in the DMN for ALFF and DC measures and in the CEN and the SN for all three fMRI measures. A close relationship between the cognitive level of the previous task and the extent of the modulation in the brain networks has been reported previously. Barnes and colleagues observed that the changes in endogenous dynamics in post-task RS is directly related to the difficulty of task performance [89]. In the case of the visual oddball paradigm used here, the levels of cognitive demand for all the three subtasks are not widely different and the whole paradigm did not require high cognitive effort. However, we observed that the extent of the changes in the RSA and local as well as global connectivity in the core RS networks in the post-task condition follows the extent of the task-induced changes within those networks. Thus, the task-induced modification of the RS activity and connectivity seems to be influenced by the intensity of the immediately preceding activation within the observed regions/networks.

A significant correlation between the behavioral outcomes in the visual oddball paradigm and the changes in the fMRI parameters could only be observed in the SN. Participants showing better performance (shorter response times in the response subtask) had a higher increase in global connectivity when comparing the second and the first RS. Thus, higher flexibility of the SN may be associated with better cognitive performance. This supports the observation that subjects with lower SN-network interactions have more pronounced inattention scores [90].

Conclusion

Our findings confirm significant dynamical changes in RSA, alongside local and global connectivity within the triple networks following a simple cognitive activity. As discussed above, the change in patterns differed noticeably between the networks and was tightly associated with the task-related brain activity. The observed changes may be an expression of the distinct involvement of the networks in the performance of the task and their various roles in the processing and integration of the immediately preceding experience. Our results provide further insight into the dynamics within and between the triple networks and contribute to a better understanding of their functional importance and interplay.

Acknowledgements

This study is considered to be part of the doctoral thesis (Dr. rer. medic.) of Mr. Hasan Sbaihat, Faculty of Medicine, RWTH Aachen University, Germany. Hasan Sbaihat would like to thank the Palestinian German Science Bridge (PGSB), Federal Ministry of Education and Research Germany, and the Palestine Academy for Science and Technology (PALAST) for their assistance and scholarship funding. The authors would like to thank Dr. Jorge Arrubla and Tracy Warbrick for their help in data acquisition, and Dr. Shivakumar Viswanathan for providing advice on statistics. Finally, authors would like to thank Ms. Claire Rick and Mr. Dennis Thomas for proofreading the manuscript.

References

1. Menon V, Uddin LQ. Saliency, switching, attention and control: a network model of insula function. Brain Struct Funct. 2010 May 29;214(5–6):655–67. doi: 10.1007/s00429-010-0262-0

2. Menon V. Large-scale brain networks and psychopathology: a unifying triple network model. Trends in Cognitive Sciences. 2011 Oct;15(10):483–506. doi: 10.1016/j.tics.2011.08.003

3. Wu X, Li Q, Yu X, Chen K, Fleisher AS, Guo X, et al. A Triple Network Connectivity Study of Large-Scale Brain Systems in Cognitively Normal APOE4 Carriers. Front Aging Neurosci. 2016 Sep 28;8. doi: 10.3389/fnagi.2016.00231

4. Krishnadas R, Ryali S, Chen T, Uddin L, Supekar K, Palaniyappan L, et al. Resting state functional hyperconnectivity within a triple network model in paranoid schizophrenia. The Lancet. 2014 Feb;383:S65. doi: 10.1016/S0140-6736(14)60328-7

5. Lin P, Yang Y, Gao J, De Pisapia N, Ge S, Wang X, et al. Dynamic Default Mode Network across Different Brain States. Sci Rep. 2017 Apr 6;7(1). doi: 10.1038/srep46088

6. Greicius MD, Krasnow B, Reiss AL, Menon V. Functional connectivity in the resting brain: A network analysis of the default mode hypothesis. Proceedings of the National Academy of Sciences. 2002 Dec 27;100(1):253–8. doi: 10.1073/pnas.0135058100

7. Greicius MD, Menon V. Default-Mode Activity during a Passive Sensory Task: Uncoupled from Deactivation but Impacting Activation. Journal of Cognitive Neuroscience. 2004 Nov;16(9):1484–92. doi: 10.1162/0898929042568532

8. van den Heuvel MP, Sporns O. Network hubs in the human brain. Trends in Cognitive Sciences. 2013 Dec;17(12):683–96. doi: 10.1016/j.tics.2013.09.012

9. Hagmann P, Cammoun L, Gigandet X, Meuli R, Honey CJ, Wedeen VJ, et al. Mapping the Structural Core of Human Cerebral Cortex. Friston KJ, editor. PLoS Biol. 2008 Jul 1;6(7):e159. doi: 10.1371/journal.pbio.0060159

10. Elton A, Gao W. Task-positive Functional Connectivity of the Default Mode Network Transcends Task Domain. Journal of Cognitive Neuroscience. 2015 Dec;27(12):2369–81. doi: 10.1162/jocn_a_00859

11. Wang Z, Liu J, Zhong N, Qin Y, Zhou H, Li K. Changes in the brain intrinsic organization in both on-task state and post-task resting state. NeuroImage. 2012 Aug;62(1):394–407. doi: 10.1016/j.neuroimage.2012.04.051

12. Li B, Wang X, Yao S, Hu D, Friston K. Task-Dependent Modulation of Effective Connectivity within the Default Mode Network. Front Psychology. 2012;3. doi: 10.3389/fpsyg.2012.00206

13. Müller NG, Knight RT. The functional neuroanatomy of working memory: Contributions of human brain lesion studies. Neuroscience. 2006 Apr;139(1):51–8. doi: 10.1016/j.neuroscience.2005.09.018

14. Bressler SL, Menon V. Large-scale brain networks in cognition: emerging methods and principles. Trends in Cognitive Sciences. 2010 Jun;14(6):277–90. doi:

10.1016/j.tics.2010.04.004

15. Li Q, Liu J, Wang W, Wang Y, Li W, Chen J, et al. Disrupted coupling of large-scale networks is associated with relapse behaviour in heroin-dependent men. jpn. 2018 Jan 1;43(1):48–57. doi: 10.1503/jpn.170011

16. Seeley WW, Menon V, Schatzberg AF, Keller J, Glover GH, Kenna H, et al. Dissociable Intrinsic Connectivity Networks for Salience Processing and Executive Control. Journal of Neuroscience. 2007 Feb 28;27(9):2349–56. doi: 10.1523/JNEUROSCI.5587-06.2007

17. Goulden N, Khusnulina A, Davis NJ, Bracewell RM, Bokde AL, McNulty JP, et al. The salience network is responsible for switching between the default mode network and the central executive network: Replication from DCM. NeuroImage]. 2014 Oct;99:180–90.doi: 10.1016/j.neuroimage.2014.05.052

18. Sridharan D, Levitin DJ, Menon V. A critical role for the right fronto-insular cortex in switching between central-executive and default-mode networks. Proceedings of the National Academy of Sciences. 2008 Aug 22;105(34):12569–74. doi: 10.1073/pnas.0800005105

19. Fox MD, Snyder AZ, Vincent JL, Corbetta M, Van Essen DC, Raichle ME. From The Cover: The human brain is intrinsically organized into dynamic, anticorrelated functional networks. Proceedings of the National Academy of Sciences. 2005 Jun 23;102(27):9673–8. doi: 10.1073/pnas.0504136102

20. Shannon BJ, Raichle ME, Snyder AZ, Fair DA, Mills KL, Zhang D, et al. Premotor functional connectivity predicts impulsivity in juvenile offenders. Proceedings of the National Academy of Sciences. 2011 Jun 27;108(27):11241–5. doi: 10.1073/pnas.1108241108

21. Chand GB, Dhamala M. Interactions Among the Brain Default-Mode, Salience, and Central-Executive Networks During Perceptual Decision-Making of Moving Dots. Brain Connectivity. 2016 Apr;6(3):249–54. doi: 10.1089/brain.2015.0379

22. Zheng H, Xu L, Xie F, Guo X, Zhang J, Yao L, et al. The Altered Triple Networks Interaction in Depression under Resting State Based on Graph Theory. BioMed Research International [Internet]. 2015;2015:1–8. doi: 10.1155/2015/386326

23. Liu Y, Li L, Li B, Feng N, Li L, Zhang X, et al. Decreased Triple Network Connectivity in Patients with Recent Onset Post-Traumatic Stress Disorder after a Single Prolonged Trauma Exposure. Sci Rep. 2017 Oct 3;7(1). doi: 10.1038/s41598-017-12964-6

24. Fan J, Zhong M, Gan J, Liu W, Niu C, Liao H, et al. Altered connectivity within and between the default mode, central executive, and salience networks in obsessive-compulsive disorder. Journal of Affective Disorders. 2017 Dec;223:106–14. doi: 10.1016/j.jad.2017.07.041

25. Manoliu A, Riedl V, Zherdin A, Mühlau M, Schwerthöffer D, Scherr M, et al. Aberrant Dependence of Default Mode/Central Executive Network Interactions on Anterior Insular Salience Network Activity in Schizophrenia. Schizophrenia Bulletin. 2013 Mar 21;40(2):428–37. doi: 10.1093/schbul/sbt037

26. Jiang L, Zuo X-N. Regional Homogeneity. Neuroscientist. 2016 Jul 9;22(5):486–505. doi: 10.1177/1073858415595004

27. Menon B. Towards a new model of understanding – The triple network, psychopathology and the structure of the mind. Medical Hypotheses. 2019 Dec;133:109385. doi: 10.1016/j.mehy.2019.109385

28. Imperatori C, Massullo C, Carbone GA, Panno A, Giacchini M, Capriotti C, et al. Increased Resting State Triple Network Functional Connectivity in Undergraduate Problematic Cannabis Users: A Preliminary EEG Coherence Study. Brain Sciences. 2020 Feb 28;10(3):136. doi: 10.3390/brainsci10030136

29. Sakoğlu Ü, Pearlson GD, Kiehl KA, Wang YM, Michael AM, Calhoun VD. A method for evaluating dynamic functional network connectivity and task-modulation: application to

schizophrenia. Magn Reson Mater Phy. 2010 Feb 17;23(5–6):351–66. doi: 10.1007/s10334-010-0197-8

30. Bassett DS, Wymbs NF, Porter MA, Mucha PJ, Carlson JM, Grafton ST. Dynamic reconfiguration of human brain networks during learning. Proceedings of the National Academy of Sciences [Internet]. 2011 Apr 18;108(18):7641–6. doi: 10.1073/pnas.1018985108

31. Albert NB, Robertson EM, Miall RC. The Resting Human Brain and Motor Learning. Current Biology. 2009 Jun;19(12):1023–7. doi: 10.1016/j.cub.2009.04.028

32. Lewis CM, Baldassarre A, Committeri G, Romani GL, Corbetta M. Learning sculpts the spontaneous activity of the resting human brain. Proceedings of the National Academy of Sciences. 2009 Oct 5;106(41):17558–63. doi: 10.1073/pnas.0902455106

33. Stevens WD, Buckner RL, Schacter DL. Correlated Low-Frequency BOLD Fluctuations in the Resting Human Brain Are Modulated by Recent Experience in Category-Preferential Visual Regions. Cerebral Cortex. 2009 Dec 21;20(8):1997–2006. doi: 10.1093/cercor/bhp270

34. Taubert M, Lohmann G, Margulies DS, Villringer A, Ragert P. Long-term effects of motor training on resting-state networks and underlying brain structure. NeuroImage. 2011 Aug;57(4):1492–8. doi: 10.1016/j.neuroimage.2011.05.078

35. Sami S, Robertson EM, Miall RC. The Time Course of Task-Specific Memory Consolidation Effects in Resting State Networks. Journal of Neuroscience. 2014 Mar 12;34(11):3982–92. doi: 10.1523/JNEUROSCI.4341-13.2014

36. Hartzell JF, Tobia MJ, Davis B, Cashdollar NM, Hasson U. Differential lateralization of hippocampal connectivity reflects features of recent context and ongoing demands: An examination of immediate post-task activity. Hum Brain Mapp. 2014 Oct 8;36(2):519–37.

doi: 10.1002/hbm.22644

37. Gregory MD, Agam Y, Selvadurai C, Nagy A, Vangel M, Tucker M, et al. Resting state connectivity immediately following learning correlates with subsequent sleep-dependent enhancement of motor task performance. NeuroImage [Internet]. 2014 Nov;102:666–73. doi: 10.1016/j.neuroimage.2014.08.044

38. Squires NK, Squires KC, Hillyard SA. Two varieties of long-latency positive waves evoked by unpredictable auditory stimuli in man. Electroencephalography and Clinical Neurophysiology. 1975 Apr;38(4):387–401. doi: 10.1016/0013-4694(75)90263-1

39. Bledowski C. Localizing P300 Generators in Visual Target and Distractor Processing: A Combined Event-Related Potential and Functional Magnetic Resonance Imaging Study. Journal of Neuroscience. 2004 Oct 20;24(42):9353–60. doi: 10.1523/JNEUROSCI.1897-04.2004

40. Gur RC, Turetsky BI, Loughead J, Waxman J, Snyder W, Ragland JD, et al. Hemodynamic responses in neural circuitries for detection of visual target and novelty: An event-related fMRI study. Hum Brain Mapp. 2007;28(4):263–74. doi: 10.1002/hbm.20319

41. Kiehl KA, Stevens MC, Laurens KR, Pearlson G, Calhoun VD, Liddle PF. An adaptive reflexive processing model of neurocognitive function: supporting evidence from a large scale (n = 100) fMRI study of an auditory oddball task. NeuroImage. 2005 Apr;25(3):899–915. doi: 10.1016/j.neuroimage.2004.12.035

42. Strobel A, Debener S, Sorger B, Peters JC, Kranczioch C, Hoechstetter K, et al. Novelty and target processing during an auditory novelty oddball: A simultaneous event-related potential and functional magnetic resonance imaging study. NeuroImage. 2008 Apr;40(2):869–83. doi: 10.1016/j.neuroimage.2007.10.065

43. Warbrick T, Mobascher A, Brinkmeyer J, Musso F, Richter N, Stoecker T, et al. Single-trial

P3 amplitude and latency informed event-related fMRI models yield different BOLD response patterns to a target detection task. NeuroImage. 2009 Oct;47(4):1532–44. doi: 10.1016/j.neuroimage.2009.05.082

44. Linden DEJ. The Functional Neuroanatomy of Target Detection: An fMRI Study of Visual and Auditory Oddball Tasks. Cerebral Cortex. 1999 Dec 1;9(8):815–23. doi: 10.1093/cercor/9.8.815

45. McCarthy G, Luby M, Gore J, Goldman-Rakic P. Infrequent Events Transiently Activate Human Prefrontal and Parietal Cortex as Measured by Functional MRI. Journal of Neurophysiology. 1997 Mar 1;77(3):1630–4. doi: 10.1152/jn.1997.77.3.1630

46. Yoshiura T, Zhong J, Shibata DK, Kwok WE, Shrier DA, Numaguchi Y. Functional MRI study of auditory and visual oddball tasks. NeuroReport. 1999 Jun;10(8):1683–8. doi: 10.1097/00001756-199906030-00011

47. Halgren E, Marinkovic K, Chauvel P. Generators of the late cognitive potentials in auditory and visual oddball tasks. Electroencephalography and Clinical Neurophysiology. 1998 Feb;106(2):156–64. doi: 10.1016/s0013-4694(97)00119-3

48. Zang Y, Jiang T, Lu Y, He Y, Tian L. Regional homogeneity approach to fMRI data analysis. NeuroImage. 2004 May;22(1):394–400. doi: 10.1016/j.neuroimage.2003.12.030

49. Zuo X-N, Ehmke R, Mennes M, Imperati D, Castellanos FX, Sporns O, et al. Network Centrality in the Human Functional Connectome. Cerebral Cortex. 2011 Oct 2;22(8):1862–75. doi: 10.1093/cercor/bhr269

50. Yu-Feng Z, Yong H, Chao-Zhe Z, Qing-Jiu C, Man-Qiu S, Meng L, et al. Altered baseline brain activity in children with ADHD revealed by resting-state functional MRI. Brain and Development. 2007 Mar;29(2):83–91. doi: 10.1016/j.braindev.2006.07.002

51. Warbrick T, Reske M, Shah NJ. Do EEG paradigms work in fMRI? Varying task demands in the visual oddball paradigm: Implications for task design and results interpretation.

NeuroImage. 2013 Aug;77:177–85. doi: 10.1016/j.neuroimage.2013.03.026

52. Smith SM. Fast robust automated brain extraction. Hum Brain Mapp. 2002 Nov;17(3):143–55. doi: 10.1002/hbm.10062

53. Jenkinson M, Bannister P, Brady M, Smith S. Improved Optimization for the Robust and Accurate Linear Registration and Motion Correction of Brain Images. NeuroImage. 2002 Oct;17(2):825–41. doi: 10.1006/nimg.2002.1132

54. Woolrich MW, Ripley BD, Brady M, Smith SM. Temporal Autocorrelation in Univariate Linear Modeling of FMRI Data. NeuroImage. 2001 Dec;14(6):1370–86. doi: 10.1006/nimg.2001.0931

55. Jenkinson M, Smith S. A global optimisation method for robust affine registration of brain images. Medical Image Analysis. 2001 Jun;5(2):143–56. doi: 10.1016/s1361-8415(01)00036-6

56. Woolrich MW, Behrens TEJ, Beckmann CF, Jenkinson M, Smith SM. Multilevel linear modelling for FMRI group analysis using Bayesian inference. NeuroImage. 2004 Apr;21(4):1732–47. doi: 10.1016/j.neuroimage.2003.12.023

57. Shirer WR, Ryali S, Rykhlevskaia E, Menon V, Greicius MD. Decoding Subject-Driven Cognitive States with Whole-Brain Connectivity Patterns. Cerebral Cortex. 2011 May 26;22(1):158–65. doi: 10.1093/cercor/bhr099

58. Yan C-G, Wang X-D, Zuo X-N, Zang Y-F. DPABI: Data Processing & Analysis for (Resting-State) Brain Imaging. Neuroinform. 2016 Apr 13;14(3):339–51. doi: 10.1007/s12021-016-9299-4

59. Yan. DPARSF: a MATLAB toolbox for “pipeline” data analysis of resting-state fMRI. Front Syst Neurosci. 2010. doi: 10.3389/fnsys.2010.00013

60. Takeuchi H, Taki Y, Nouchi R, Sekiguchi A, Hashizume H, Sassa Y, et al. Degree centrality and fractional amplitude of low-frequency oscillations associated with Stroop interference.

NeuroImage. 2015 Oct;119:197–209. doi: 10.1016/j.neuroimage.2015.06.058

61. Gideon RA. The Correlation Coefficients. J Mod App Stat Meth. 2007 Nov 1;6(2):517–29. doi: 10.22237/jmasm/1193890500

62. Zou Q-H, Zhu C-Z, Yang Y, Zuo X-N, Long X-Y, Cao Q-J, et al. An improved approach to detection of amplitude of low-frequency fluctuation (ALFF) for resting-state fMRI: Fractional ALFF. Journal of Neuroscience Methods. 2008 Jul;172(1):137–41. doi: 10.1016/j.jneumeth.2008.04.012

63. McKiernan KA, Kaufman JN, Kucera-Thompson J, Binder JR. A Parametric Manipulation of Factors Affecting Task-induced Deactivation in Functional Neuroimaging. Journal of Cognitive Neuroscience. 2003 Apr 1;15(3):394–408. doi: 10.1162/089892903321593117

64. Pyka M, Beckmann CF, Schöning S, Hauke S, Heider D, Kugel H, et al. Impact of Working Memory Load on fMRI Resting State Pattern in Subsequent Resting Phases. Lauwereyns J, editor. PLoS ONE. 2009 Sep 25;4(9):e7198. doi: 10.1371/journal.pone.0007198

65. Tommasin S, Mascali D, Gili T, Eid Assan I, Moraschi M, Fratini M, et al. Task-Related Modulations of BOLD Low-Frequency Fluctuations within the Default Mode Network. Front Phys. 2017 Jul 25;5. doi: 10.3389/fphy.2017.00031

66. Mason MF, Norton MI, Van Horn JD, Wegner DM, Grafton ST, Macrae CN. Wandering Minds: The Default Network and Stimulus-Independent Thought. Science. 2007 Jan 19;315(5810):393–5. doi: 10.1126/science.1131295

67. Thomason ME, Chang CE, Glover GH, Gabrieli JDE, Greicius MD, Gotlib IH. Default-mode function and task-induced deactivation have overlapping brain substrates in children. NeuroImage [Internet]. 2008 Jul;41(4):1493–503. doi: 10.1016/j.neuroimage.2008.03.029

68. Zuo X-N, Xu T, Jiang L, Yang Z, Cao X-Y, He Y, et al. Toward reliable characterization of functional homogeneity in the human brain: Preprocessing, scan duration, imaging resolution and computational space. NeuroImage. 2013 Jan;65:374–86. doi:

10.1016/j.neuroimage.2012.10.017

69. Zuo X-N, Xing X-X. Test-retest reliabilities of resting-state FMRI measurements in human brain functional connectomics: A systems neuroscience perspective. Neuroscience & Biobehavioral Reviews. 2014 Sep;45:100–18. doi: 10.1016/j.neubiorev.2014.05.009

70. Lee T-W, Xue S-W. Linking graph features of anatomical architecture to regional brain activity: A multi-modal MRI study. Neuroscience Letters. 2017 Jun;651:123–7. doi: 10.1016/j.neulet.2017.05.005

71. Respino M, Hoptman MJ, Victoria LW, Alexopoulos GS, Solomonov N, Stein AT, et al. Cognitive Control Network Homogeneity and Executive Functions in Late-Life Depression. Biological Psychiatry: Cognitive Neuroscience and Neuroimaging. 2020 Feb;5(2):213–21. doi: 10.1016/j.bpsc.2019.10.013

72. Craig AD. How do you feel? Interoception: the sense of the physiological condition of the body. Nat Rev Neurosci. 2002 Aug;3(8):655–66. doi: 10.1038/nrn894

73. Critchley HD, Wiens S, Rotshtein P, Öhman A, Dolan RJ. Neural systems supporting interoceptive awareness. Nat Neurosci. 2004 Jan 18;7(2):189–95. doi: 10.1038/nn1176

74. Sridharan D, Levitin DJ, Menon V. A critical role for the right fronto-insular cortex in switching between central-executive and default-mode networks. Proceedings of the National Academy of Sciences. 2008 Aug 22;105(34):12569–74. doi: 10.1073/pnas.0800005105

75. Liu C-H, Guo J, Lu S-L, Tang L-R, Fan J, Wang C-Y, et al. Increased Salience Network Activity in Patients With Insomnia Complaints in Major Depressive Disorder. Front Psychiatry. 2018 Mar 20;9. doi: 10.3389/fpsyt.2018.00093

76. Petrides M. Lateral prefrontal cortex: architectonic and functional organization. Phil Trans R Soc B. 2005 Apr 29;360(1456):781–95. doi: 10.1098/rstb.2005.1631

77. Akiki TJ, Averill CL, Abdallah CG. A Network-Based Neurobiological Model of PTSD:

Evidence From Structural and Functional Neuroimaging Studies. Curr Psychiatry Rep. 2017 Sep 19;19(11). doi: 10.1007/s11920-017-0840-4

78. Turner BM, Rodriguez CA, Liu Q, Molloy MF, Hoogendijk M, McClure SM. On the Neural and Mechanistic Bases of Self-Control. Cerebral Cortex. 2018 Jan 24;29(2):732–50. doi: 10.1093/cercor/bhx355

79. Gagnepain P, Hulbert J, Anderson MC. Parallel Regulation of Memory and Emotion Supports the Suppression of Intrusive Memories. J Neurosci. 2017 May 30;37(27):6423–41. doi: 10.1523/JNEUROSCI.2732-16.2017

80. Wessing I, Rehbein MA, Postert C, Fürniss T, Junghöfer M. The neural basis of cognitive change: Reappraisal of emotional faces modulates neural source activity in a frontoparietal attention network. NeuroImage [Internet]. 2013 Nov;81:15–25. doi: 10.1016/j.neuroimage.2013.04.117

81. Chen AC, Oathes DJ, Chang C, Bradley T, Zhou Z-W, Williams LM, et al. Causal interactions between fronto-parietal central executive and default-mode networks in humans. Proceedings of the National Academy of Sciences. 2013 Nov 18;110(49):19944–9. doi: 10.1073/pnas.1311772110

82. Andrews-Hanna JR, Smallwood J, Spreng RN. The default network and self-generated thought: component processes, dynamic control, and clinical relevance. Ann NY Acad Sci. 2014 Feb 6;1316(1):29–52. doi: 10.1111/nyas.12360

83. Gerlach KD, Spreng RN, Gilmore AW, Schacter DL. Solving future problems: Default network and executive activity associated with goal-directed mental simulations. NeuroImage. 2011 Apr;55(4):1816–24. doi: 10.1016/j.neuroimage.2011.01.030

84. Meyer ML, Spunt RP, Berkman ET, Taylor SE, Lieberman MD. Evidence for social working memory from a parametric functional MRI study. Proceedings of the National Academy of Sciences. 2012 Jan 23;109(6):1883–8. doi: 10.1073/pnas.1121077109

85. Beaty RE, Benedek M, Barry Kaufman S, Silvia PJ. Default and Executive Network Coupling Supports Creative Idea Production. Sci Rep. 2015 Jun 17;5(1). doi: 10.1038/srep10964

86. Spreng RN, Sepulcre J, Turner GR, Stevens WD, Schacter DL. Intrinsic Architecture Underlying the Relations among the Default, Dorsal Attention, and Frontoparietal Control Networks of the Human Brain. Journal of Cognitive Neuroscience. 2013 Jan;25(1):74–86. doi: 10.1162/jocn_a_00281

87. Chang C, Glover GH. Time–frequency dynamics of resting-state brain connectivity measured with fMRI. NeuroImage. 2010 Mar;50(1):81–98. doi: 10.1016/j.neuroimage.2009.12.011

88. Dosenbach NUF, Visscher KM, Palmer ED, Miezin FM, Wenger KK, Kang HC, et al. A Core System for the Implementation of Task Sets. Neuron. 2006 Jun;50(5):799–812. doi: 10.1016/j.neuron.2006.04.031

89. Barnes A, Bullmore ET, Suckling J. Endogenous Human Brain Dynamics Recover Slowly Following Cognitive Effort. Brembs B, editor. PLoS ONE. 2009 Aug 14;4(8):e6626. doi: 10.1371/journal.pone.0006626

90. Cai W, Chen T, Szegletes L, Supekar K, Menon V. Aberrant Time-Varying Cross-Network Interactions in Children With Attention-Deficit/Hyperactivity Disorder and the Relation to Attention Deficits. Biological Psychiatry: Cognitive Neuroscience and Neuroimaging. 2018 Mar;3(3):263–73. doi: 10.1016/j.bpsc.2017.10.005

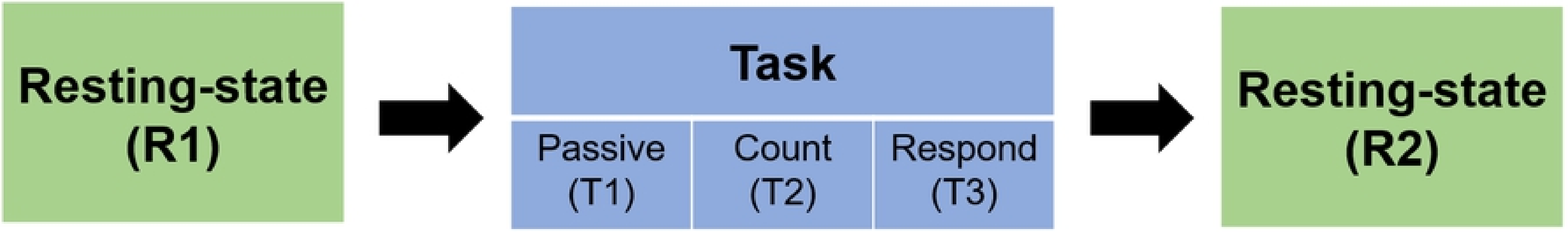
Resting-state
(R1)
Task
Passive
(T1)
Count
(T2)
Respond
(T3)
Resting-state
(R2)

Fig1

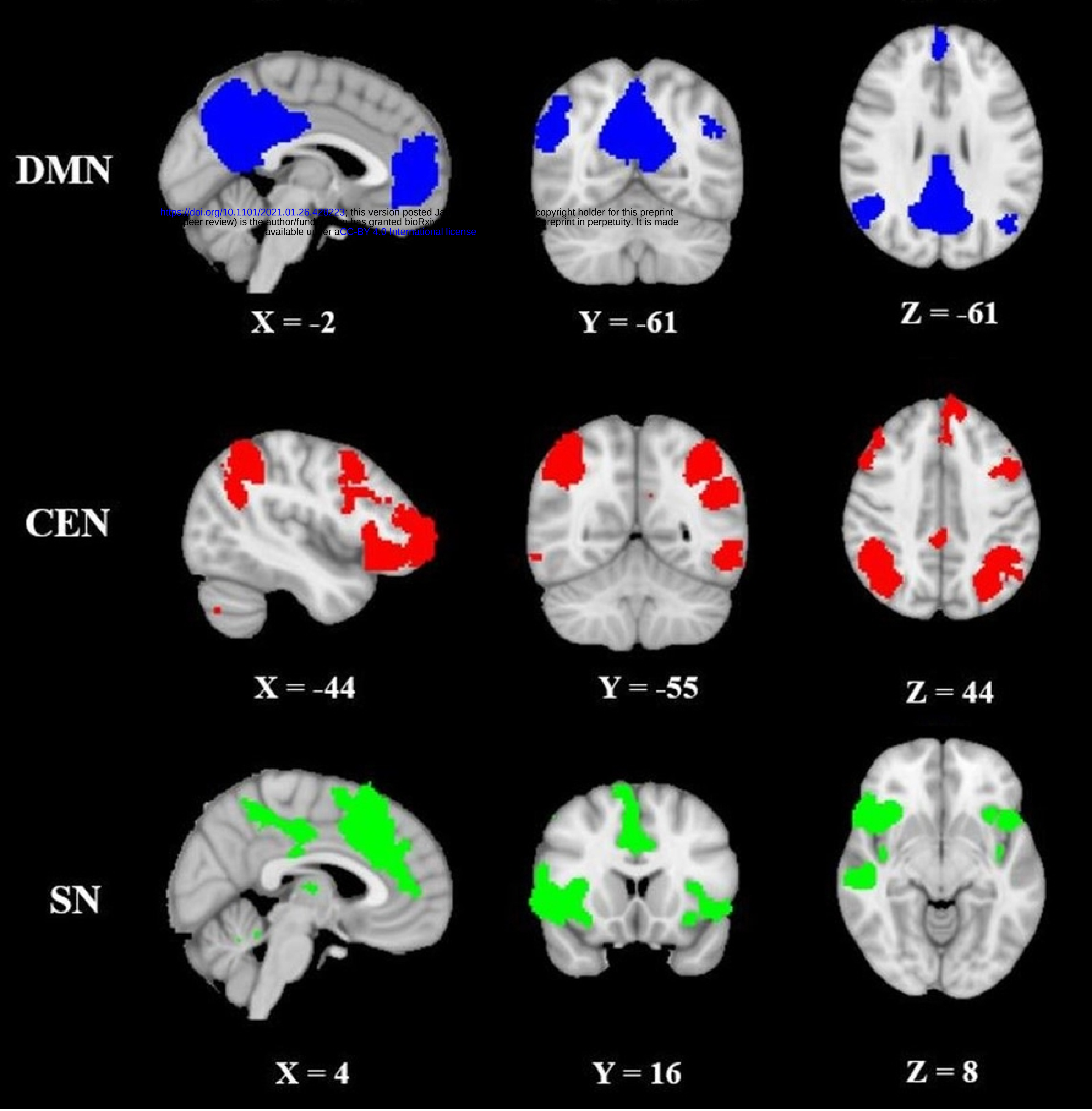

Fig2

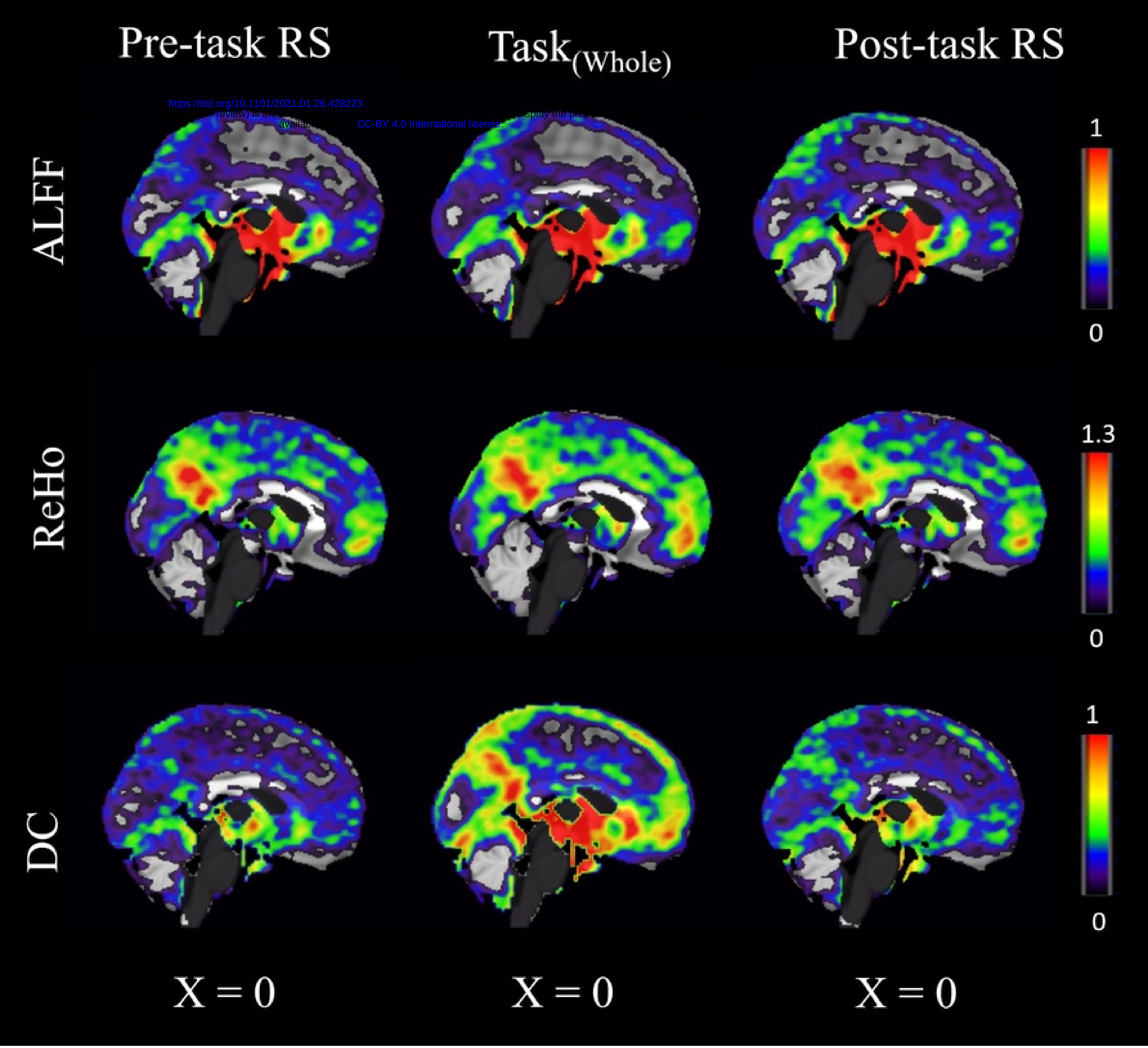
Pre-task RS
Task(Whole)
Post-task RS
ALFF
ReHo
DC
1
0
1.3
0
1
0
X = 0
X = 0
X = 0

Fig3

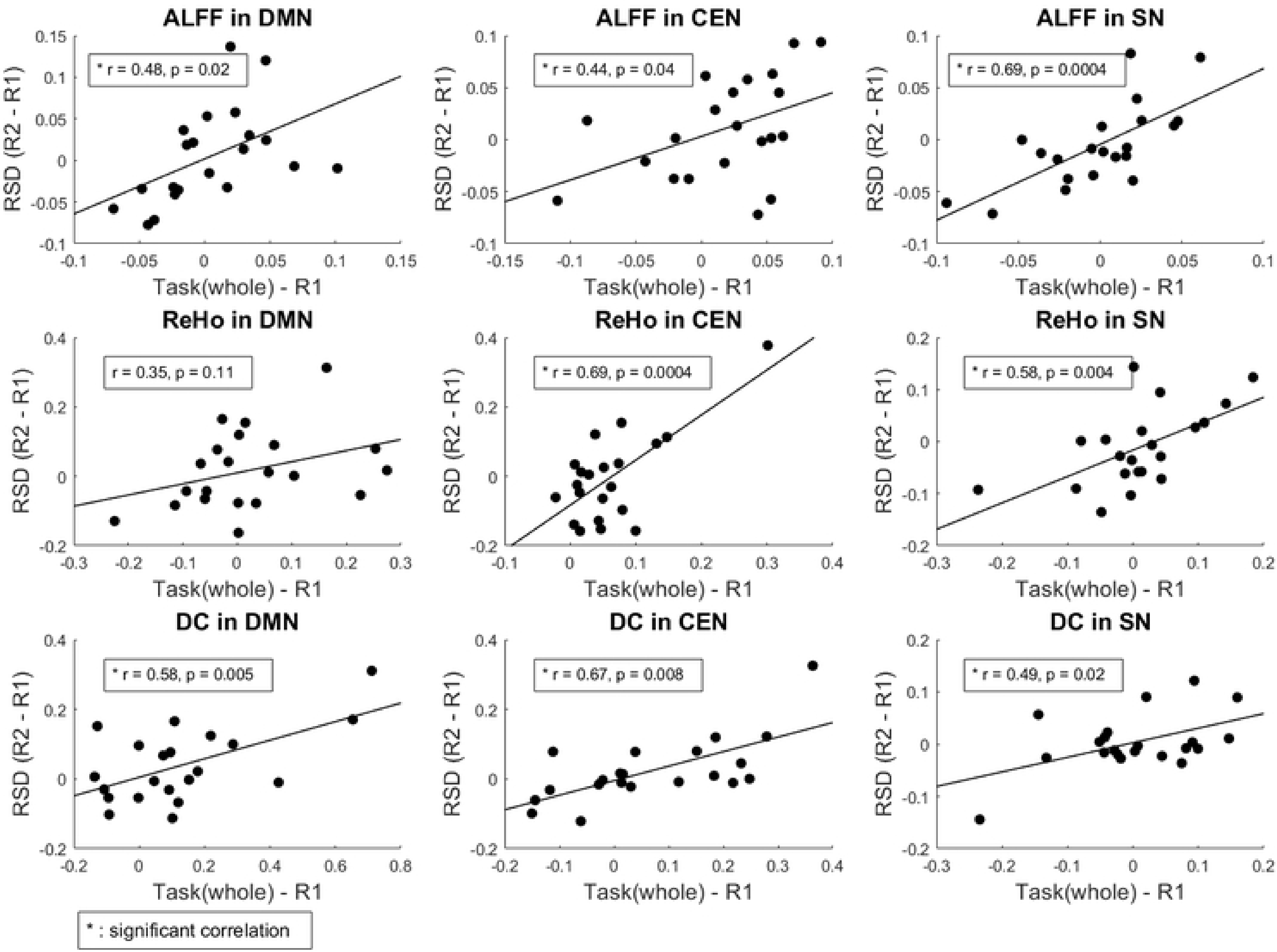
ALFF in DMN
* r = 0.48, p = 0.02
ALFF in CEN
* r = 0.44, p = 0.04
ALFF in SN
* r = 0.69, p = 0.0004
ReHo in DMN
r = 0.35, p = 0.11
ReHo in CEN
* r = 0.69, p = 0.0004
ReHo in SN
* r = 0.58, p = 0.004
DC in DMN
* r = 0.58, p = 0.005
DC in CEN
* r = 0.67, p = 0.008
DC in SN
* r = 0.49, p = 0.02
RSD (R2 - R1)
Task(whole) - R1
* : significant correlation

Fig4

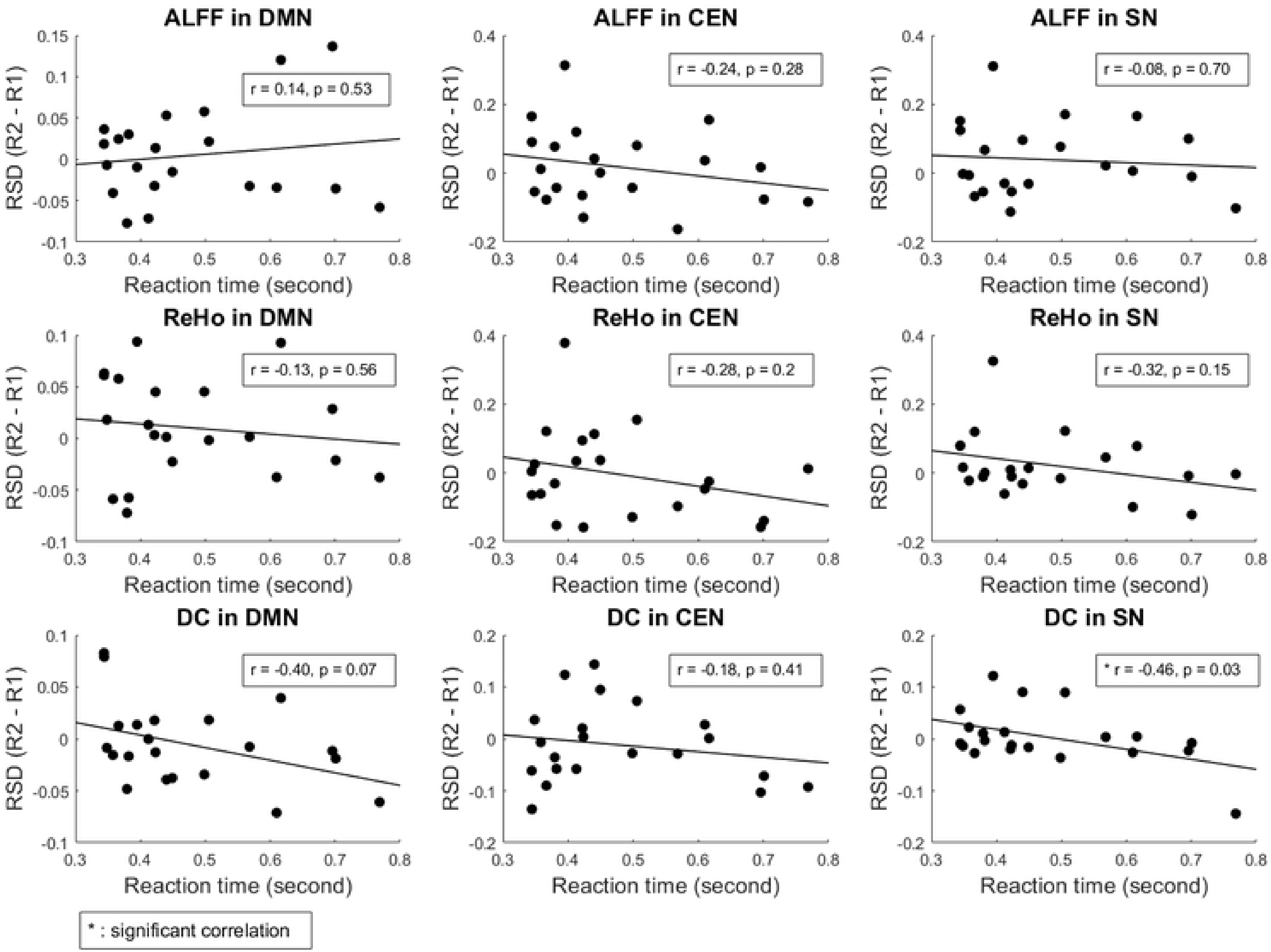

ALFF in DMN
r = 0.14, p = 0.53
ALFF in CEN
r = -0.24, p = 0.28
ALFF in SN
r = -0.08, p = 0.70
ReHo in DMN
r = -0.13, p = 0.56
ReHo in CEN
r = -0.28, p = 0.2
ReHo in SN
r = -0.32, p = 0.15
DC in DMN
r = -0.40, p = 0.07
DC in CEN
r = -0.18, p = 0.41
DC in SN
* r = -0.46, p = 0.03
RSD (R2 - R1)
Reaction time (second)
* : significant correlation

Fig5

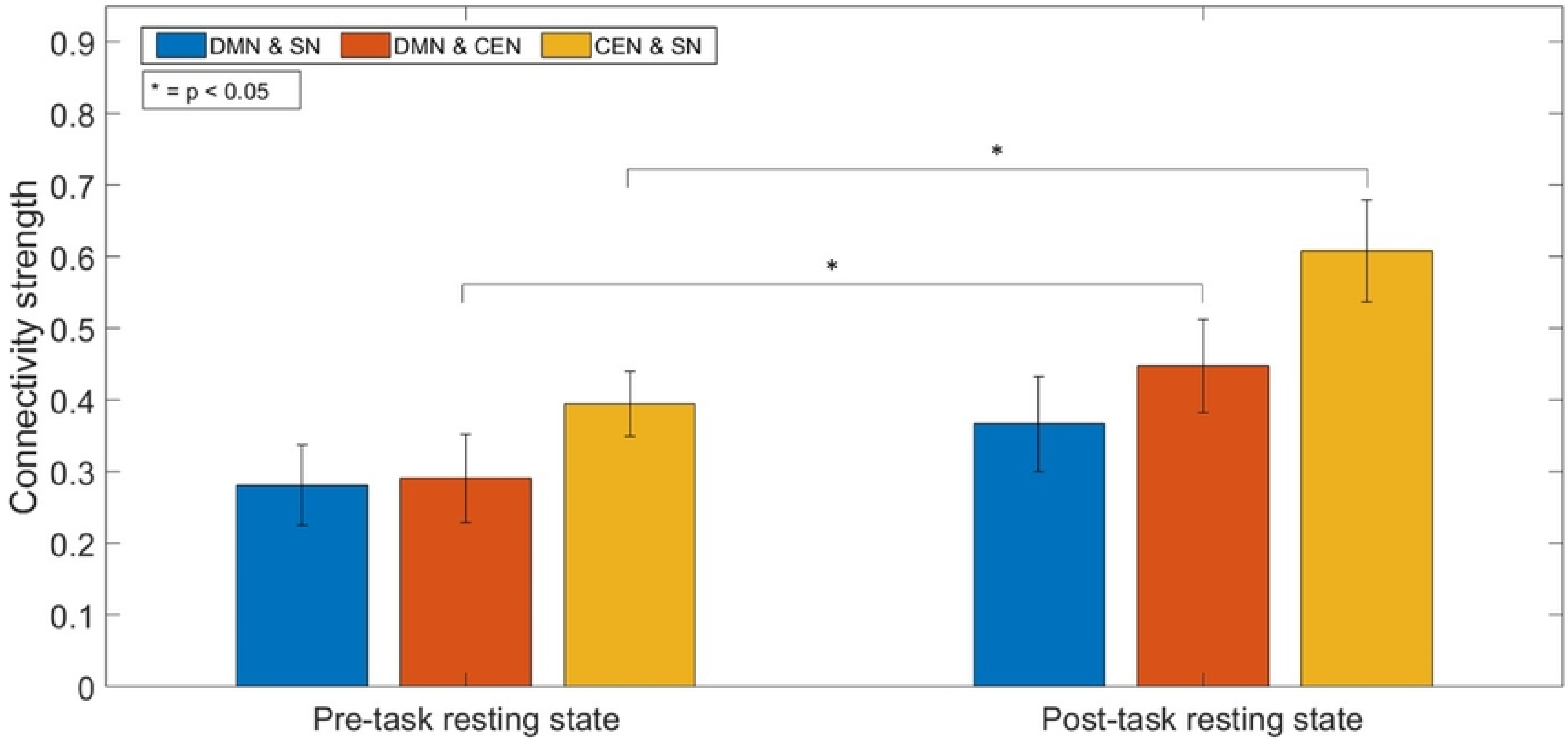

DMN & SN
DMN & CEN
CEN & SN
* = p < 0.05
Connectivity strength
0.9
0.8
0.7
0.6
0.5
0.4
0.3
0.2
0.1
0
*
*
Pre-task resting state
Post-task resting state

Fig6